Egypt. J. Geo. **Vol. 68,** pp: 219-232 (2024)

Egyptian Journal of Geology

https://egjg.journals.ekb.eg

Pre-Miocene Subsurface Structure Imaging Using Seismic and High-Resolution Aeromagnetic Data, South East Ghara in South Gulf of Suez

Shaimaa Abd El Raheem[1], Sami Abd El Nabi[2], Azza El Rawy[2] and **Khaled Khalifa[1]**

(1) Agreements and Exploration Department, South Valley Egyptian Petroleum Holding Company, P.o Box 3011 Horia, Nasr City, Cairo, Egypt

(2)Geophysics Department, Faculty of Science, Ain Shams University, P.o Box 11566, Abbasia, Cairo, Egypt

THIS PAPER sheds light on imaging of subsurface structure of South East Ghara in South Gulf of Suez based mainly on the analysis of aeromagnetic and seismic data. Since, there are several problems in South East Ghara regard to the hydrocarbon exploration. For example, the facies change in the same reservoir along the study area, which refers to the same age, complex compositions and their impact on the presence of oil gathering, and other reasons, which led to study and image the structure of the area.

The analysis strategy included, firstly magnetic based basement tectonic analysis to illustrate the detailed structures of basement complex. Secondly magnetic and seismic based depth structural mapping. The results show the basement surface configuration as well as (Nubia, Matulla, Nukhul, Rudeis, Kareem, Belayim, South Gharib and Zeit); most of them are dissected with nine clysmic normal faults. The basement tectonics analysis indicated that the area affected with dip-slip faults that considered the main cause of forming of the tilted faulted blocks in the study area and have trend NNW-SSE to NW-SE. One of these tilted faulted block forms the horst structure trend which separates between the Ghara basin and Eastern basin. The ENE-WSW to NE-SW trending faults are interpreted as probable strike-slip faults that represent the younger faults. The depth mapping based on interpretation of seismic data for three horizons (basement complex, Nubia, Matulla) show that the interpreted depth values ranged from 16500, 16400, 14400 ft subsea in its deepest point located in the northwest, and 4700, 4600, 4500 ft subsea in its shallowest point in the southeast of the study area, respectively. Based on the information extracted from drilled wells and the structure analysis, the study suggests presence two promising localities (leads) and three prospects in Nubia and Matulla formations.

Keywords: 2D seismic interpretation, aeromagnetic data analysis; structural imaging; South East Ghara.

1. Introduction

One of the best instances of integrating outcrop and subsurface data to improve hydrocarbon exploration and exploitation is the Gulf of Suez basin, which is Egypt's most productive oil province (Schlumberger 1984; Gawthorpe et al. 1990; Patton et al. 1994; Sharp et al. 2000 a & b). It forms the northern extension of the Red Sea, covering an area of about 25,000 km^2 at an average water depth of 55 to 100m (Schlumberger 1984), extends NW and located between latitudes 27o 30' 00" N to 30o 00' 00" N. This rift basin is bounded by two main bounding normal faults from both sides, which characterized by lines of high vertical escarpments on the up thrown sides (Said 1962).

The complex structures in the Gulf of Suez make subsurface study dramatically tough. In addition, there is a layer of salt of relatively large thickness, which affects seismic measurements. Companies are trying hard to reduce dry wells percentage by further understanding of geological settings. There are several problems in South East Ghara regard to the hydrocarbon exploration. For example, the facies change in the same reservoir along the study area, which refers to the same age, complex compositions and their impact on the presence of oil gathering, and other reasons, which led us to study the structure of the area.

The study area of South East Ghara lies in South Gulf of Suez, between latitudes 27° 38' 27" N - 27° 57' 46" N and longitudes 33° 44' 33" E - 34° 00' 10" E, and cover an area of about 480 km^2 (Fig. 1). It is located beneath water depth ranges from 30 feet to 700 feet (GUPCO 1980s, 2010s) and includes North Shedwan 2 & 3 oil Fields which are being operated by General Petroleum Company (GPC) and Shoab Ali oil Field which is being operated by The Gulf of Suez Petroleum Company (GUPCO).

The producing reservoirs in Shoab Ali oil Field are Pre-Cambrian (basement rocks), Pre-Miocene

*Corresponding author e-mail: shaimaa83.a@gmail.com
Received: 01/07/2024; Accepted: 21/07/2024
DOI: 10.21608/EGJG.2024.300715.1081

(Nubia, Matulla and Thebes formations) and Miocene (Nukhul, Rudies, Kareem and Belayim formations (E.G.P.C. 1996). The producing reservoir in North Shedwan-2 oil Field is Rudies formation in Miocene age, while in North Shedwan-3 oil field is Nubia formation in Pre-Miocene age (GUPCO, 1982 & 2007). The study aims to investigate structural geology and possibilities of hydrocarbon trapping in South East Ghara open area based on the integration of seismic and high resolution aeromagnetic data to construct a detailed structural framework based on 2D seismic and high resolution aeromagnetic data analysis.

The first discovery in Shoab Ali oil field was announced in 1977 after drilling of Alma-2 Well which encountered 400 feet of Miocene sand net oil pay in the interval between 4,700 and 5,500 feet subsea, which flowed 7324 barrels of oil per day during a production test. Gupco began field operations and drilled five producers' wells from the new platform “C” to the northwest of the proven field. Production from the field started with 12,000 barrels of oil per day in 1978 (E.G.P.C. 1996). In 1982, GH385-1 Well was drilled by Amoco Co. and recorded heavy oil in Lower Rudeis (GUPCO 1982). In 1982-1983, several wells were drilled in the area such as GH395-1, GH421-1, GH 386-1, GH 386-1A, GH451-1&1B and GH452-1 which was completed as the GH452-1A after the stucking of pipe. GH452-1A well tested oil in Belayim dolomite, it did establish a sharp oil water contact of 4102 feet subsea in the base of Belayim Formation. The test results of production rate are 2000 barrels of oil per day.

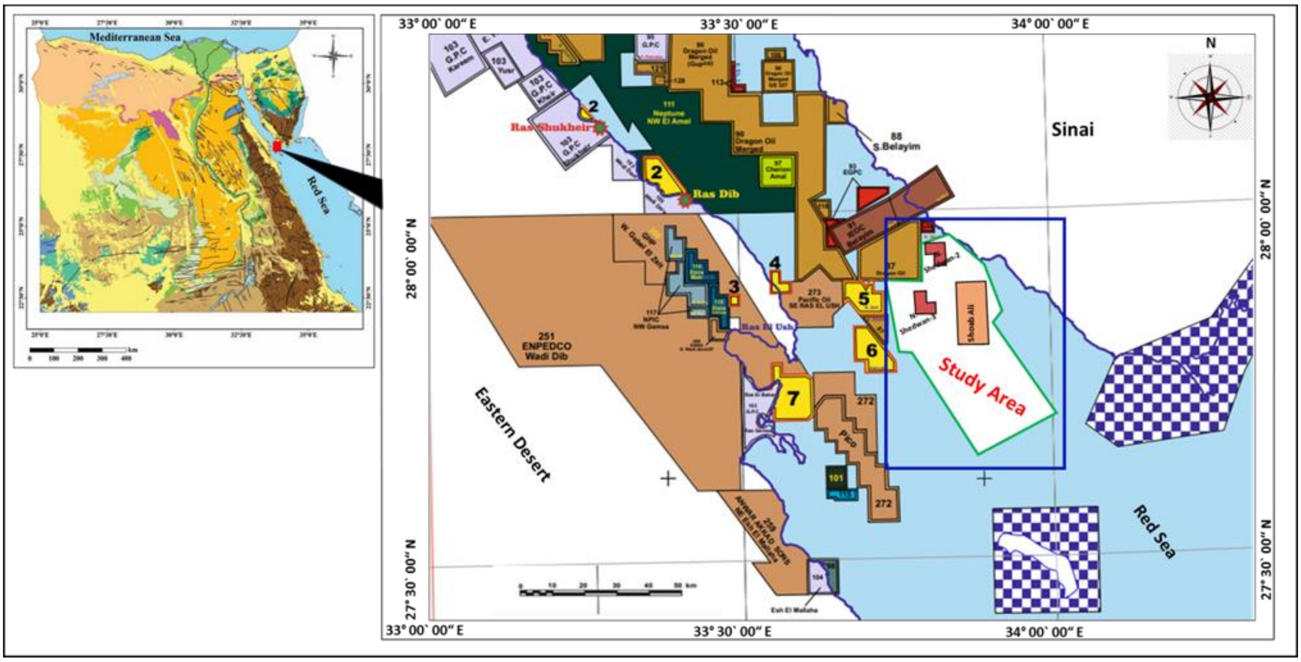

Fig. 1. Location map of South East Ghara area, South Gulf of Suez, Egypt (after EGPC, 2023).

It was classified after testing as plugged and abandoned with oil shows in the Belayim Formation (GUPCO 1984). From 1983 till 1988, several dry wells were drilled within the exploration area which are GH397-1, GH 423-1, GH 440-1, GH 434-1C, GH 420-1 and GH408-1. In 1995, the South East Gulf of Suez Concession was awarded to Repsol Exploration Egipto S.A and Penzoil Egypt, INC by law no. 17/1995. Repsol drilled SEGOS-1 and SEGOS-2 between 1997 and 2000, the two wells were dry. In 2004, North Shedwan Concession was awarded to BP Exploration (Delta) limited, by law no. 160/2004. In 2007, NS394-1 well was drilled and encountered Matulla oil pay then NS394-1A sidetrack well drilled with 200 feet of net oil pay of Nubia and oil discovery was announced by the well NS394-1A where 9 km^2 was converted to N. Shedwan-3 development lease in 01/2012. In 2008, oil discovery was announced in Lower Rudies by well GH385-1(NS385-1) which drilled in 1982 by Amoco Co., and 12 km^2 was converted to N. Shedwan-2 development lease. In 2008, NS394-2, NS394-2A and NS394-2B wells were drilled where NS394-2B recorded 49.5 feet net pay in Nubia. In 2009, NS394-3 well was drilled and classified dry hole then in 2013, NS394-4 well was drilled and classified Plugged and abandoned with some oil shows in Matulla. In 2016, N. Shedwan-2 & 3 development leases were assigned to the E.G.P.C. then awarded to GPC in 2023.

2. Geological setting

The structural framework and lithostratigraphic aspects of the southern Gulf of Suez (Fig. 2) have discussed in many literatures (e.g. Tromp, 1950; Said, 1962; Harper, 1966; Meshref et al., 1976; Barakat, 1982; E.G.P.C., 1996; Sharp et al. 2000a; Bosworth and McClay, 2001; Alsharhan, 2003; GUPCO, 1982; GUPCO, 1984 ; Abd El-Naby et al., 2009; GUPCO, 2013; Rohais et al. 2016; Bosworth and Durocher 2017; Segev et al. 2017; Temraz and Dypvik 2018).

Interpretation of geological and geophysical data indicates that the Gulf of Suez consists of elongated troughs containing several submarine ridges (elongated structural highs). As with the Gulf of Suez, both troughs and highs follow a similar pattern (NW-SE). NE-SW and ENE-WSW discordant elements separate these highs. As a result of these later elements, highs are segmented by cross faults.

Several models were developed as a result of literature discussing the tectonics of the Gulf of Suez. The first model views the Gulf of Suez as a significant graben that was generated by tension. The Gulf of Suez's development is explained by compressional stress in a second theory. A third viewpoint, however, contends that the Red Sea-Gulf of Suez split was created by the simultaneous subsidence and elevation of several fault blocks. According to a fourth opinion, the Gulf of Suez formed as a result of strike-slip faulting and regional updoming.

The Gulf of Suez has been subdivided into three tectonic provinces, which from north to south are Galala, Belayim and Morgan provinces. Three major tectonic dip provinces, separated by two northeasterly trending hinge zones were define; the Galala-Abu Zenima accommodation zone (GAZAZ) in the north and the Morgan accommodation zone (MAZ) in the south separate the northern Araba dip province (SW dips), the central Belayim dip province (NE dips) and the southern Amal-Zeit dip province (SW dips). The study area represents a part of the MAZ located in the southern part of the central Belayim province and the northern part of the Amal - Zeit province (Fig. 2).

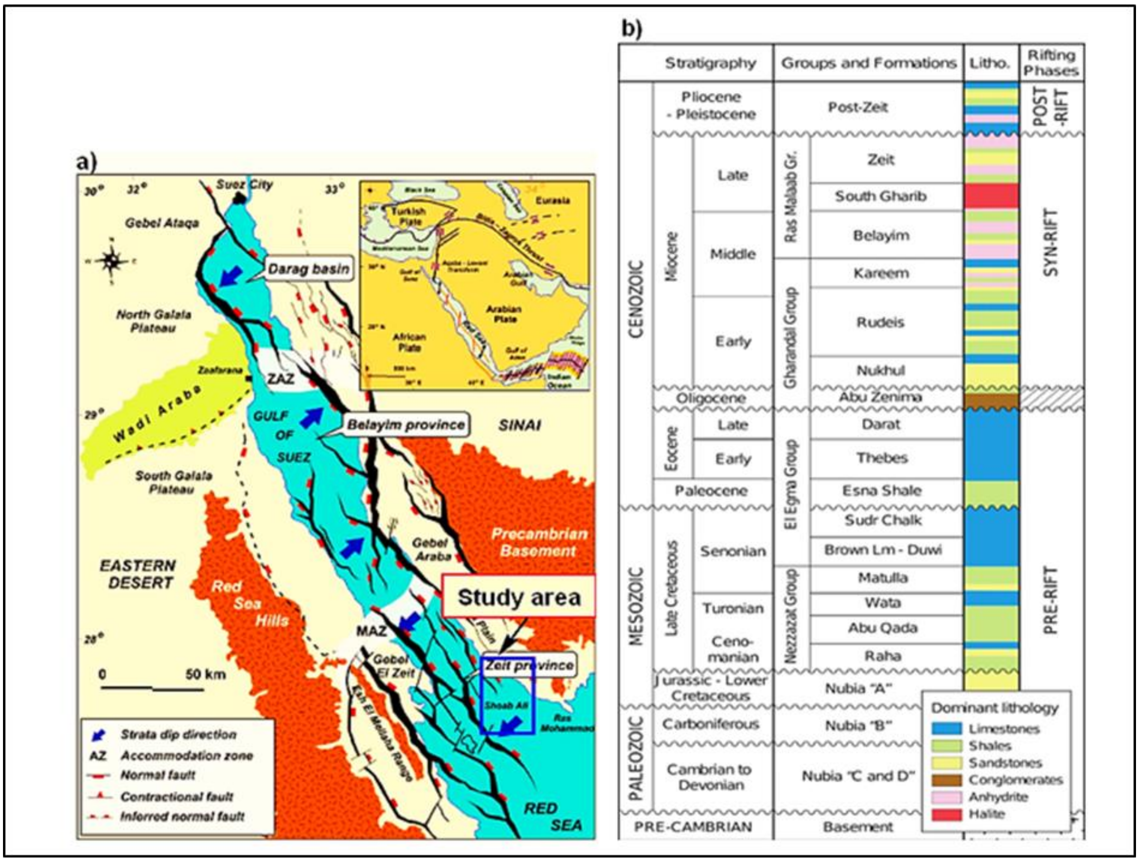

Fig. 2. Gulf of Suez tectonic map depicting major faults and accommodation zones (Bosworth and Mcclay, 2001, El Diasty et al., 2020, Radwan et al., 2020, Radwan and Sen., 2021), and b) A generalized litho-stratigraphic column for the southern Gulf of Suez, Egypt. (E.G.P.C. 1996, Radwan 2018, and Radwan et al. 2021).

The lithostratigraphic sequence of South East Ghara is shown in Figure (3), it consists of pre-rift and syn-rift sediments. Sedimentation during Pre-Rift was affected by major geologic unconformities at different geologic times and range in thickness from 25 to 430 m in the southern part. Pre-Rift sediments include basement complex, Nubia, Matulla, Brown Limestone, Sudr, Esna, and Thebes formations. This strata is composed of shale, sandstone, limestone, carbonates clays, siltstone. According to the petrophysical and structural studies, there are observed that the granitic rocks formed the basement in the study area. Tectonic activity in this region has caused the basement to become highly weathered and fractured. Brown Limestone formation exhibits depth about 11000 feet in the northwestern part of the area of interest. Sudr formation is consisted of carbonates and clays and exhibits deeper depth in the western part. Esna formation is composed of marly, and highly fossiliferous in the southern part of the study area. Thebes formation is composed of marl, with calcareous gray shale with average thickness about 40 feet.

Syn-rift stratigraphic sequence includes Nukhul, Rudeis, Kareem, Belayim, South Gharib, Zeit, Post Zeit formations. Sedimentation during this period mainly consists of sandstone with limestone, shale streaks, markha anhydrite in the southern Gulf of Suez. A carbonate and shale section at the top of the upper Rudies formation caps the sandstone with thin shale beds of the lower Rudies formation. Gypsum, halite, and anhydrite composed the South Gharib and Zeit formations, and the Belayim main lithology is composed of anhydrite, carbonates, and gypsum (Abd-Allah et al., 2014).

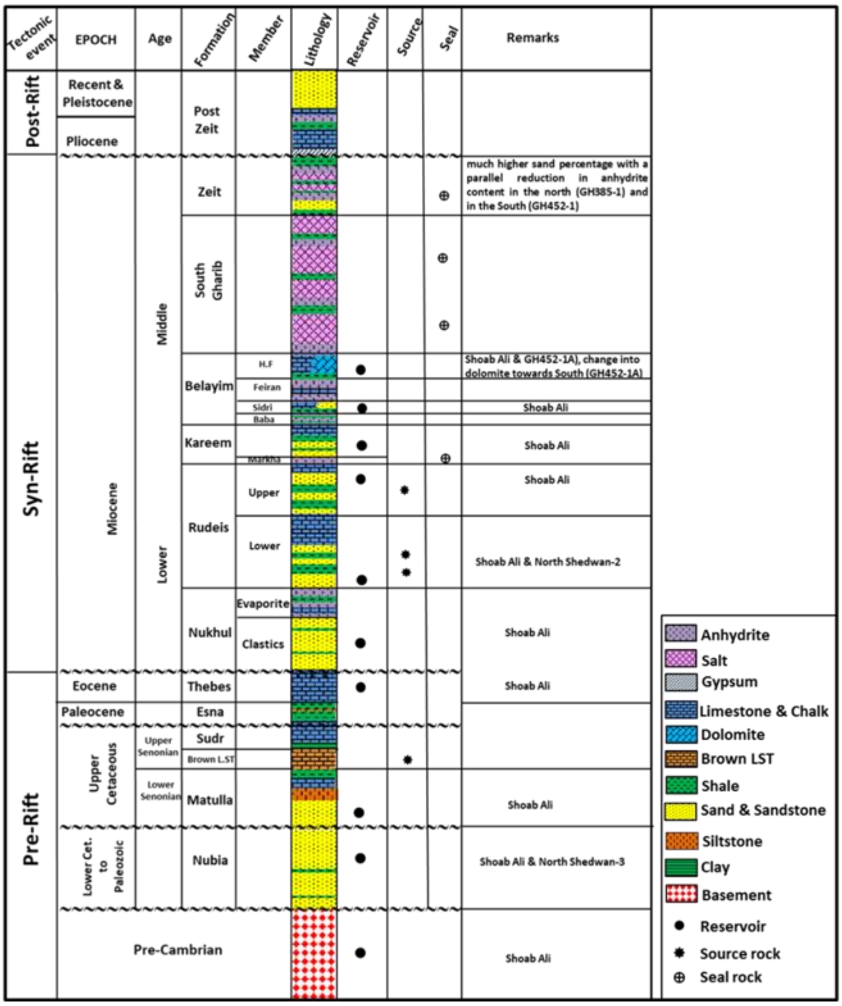

Fig. 3. A generalized litho-stratigraphic column of the South East Ghara area, South Gulf of Suez, Egypt. (Modified after, E.G.P.C. 1996).

3. Datasets

The methods and material used in the study (high resolution aeromagnetic, seismic, and well data).

3.1. Aeromagnetic Data

High-resolution aeromagnetic data was acquired by CGG Company and processed 1997. The flying pattern were a 250m spacing between flight lines (at azimuth N60°W) and 400-m spacing between tie lines (perpendicular to the flight lines). Nominal flying elevation was 100 m above sea level. A high-resolution aeromagnetic data covered the study area and extended to the east. The flight path map included the boundary of the area of interest (blue block) is shown in Figure (4). The total magnetic intensity (TMI) grid was created for the survey area using a Bi-Directional line gridding algorithm and grid cell size of 50 x 50 m as shown in Figure (5). Used software is Geosoft 2008.

3.2. Seismic and Well Data

About 450 km^2 of 3D seismic data covers the study area was acquired by BP/GUPCO, (2013). Used software is Petrel-2017

Also, four wells (GH385-1, NS394-1 & 1A, SA-E8 and GH452-1A) used in this study (Fig. 4). These wells were targeted the Miocene (Nukhul, Rudeis, and Belayim) reservoirs and Pre-Miocene Nubia formation. The wells NS394-1 & NS394-1A, SA-E8 and GH452-1A penetrated basement at depths 11738, 11035, 5474 and 5482 ft subsea respectively while GH385-1 penetrated Matulla at subsea depth 8173.

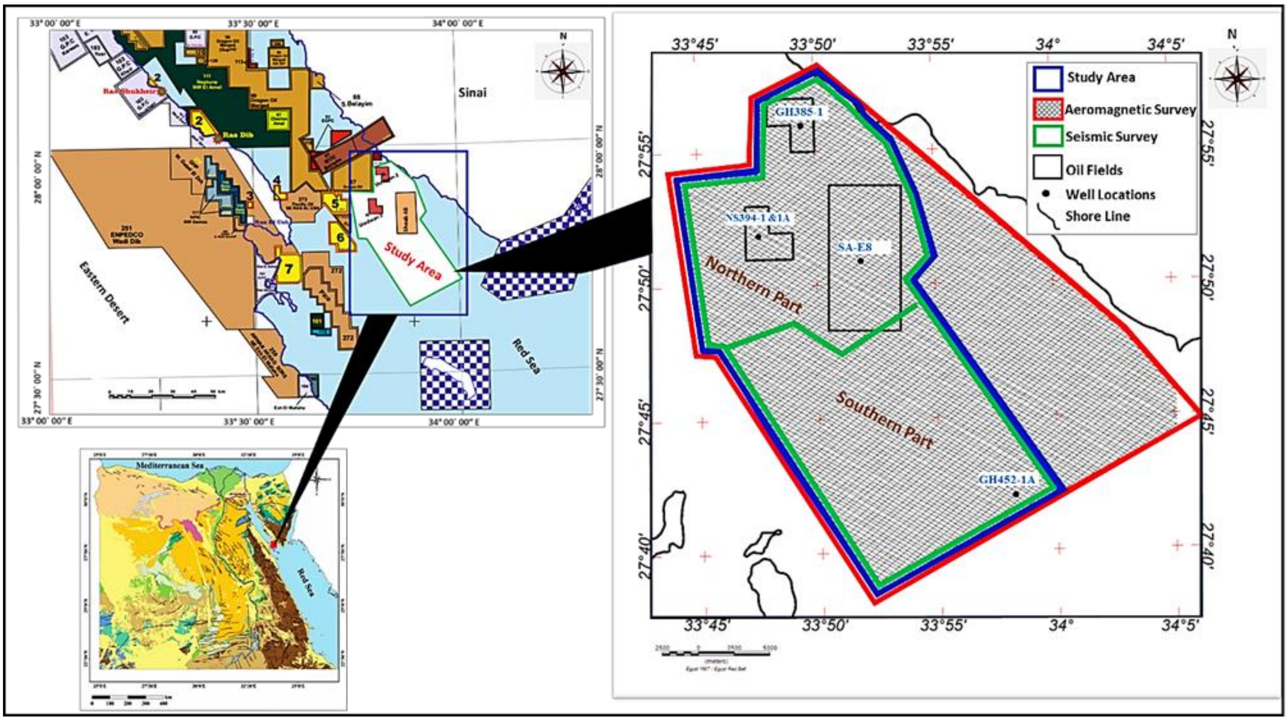

Fig. 4. The available data of South East Ghara, South Gulf of Suez, Egypt. The area of interest is shown within the blue boundary.

4. Data Interpretation

Analyzing and interpreting data involves several steps. The seismic data are examined independently from wells data. Vertical seismic profiles (VSP) are used to define the exact time for the depositional horizons of interest. The initial step in the seismic interpretation process is to tie geological horizons to seismic reflectors. In the next step, seismic horizons is selected by character continuity and structural elements and detected using Petrel software 2017. The most important in this process is to follow a loop that allows us to check the reflectors interpretation. The two lines, at an intersection at the same place, must agree there. The last stage of 2D seismic interpretation is locating important fault patterns, and calculating and contouring the depth values of important horizons including the top of the basement, as well as Nubia, and Matulla formations.

On the other hand, the analysis of aeromagnetic data comprises two parts. Firstly, determining lineament patterns for different physical depths, in order to gain a three-dimensional appreciation of structure. This is performed though applied Fourier

Gaussian filters to the observed data to separate the magnetic anomalies by apparent source depths. The first vertical derivative (FVD) and the tilt derivative (TDR) techniques are applied to RTP and its magnetic components data of the study area to amplify short-wavelength information and to emphasize edges of potential field sources. Secondly, determining depths to basement relief. Subsurface information of wells data, apparent susceptibility and seismic interpretation are used to help constrain the interpreted basement structure and depth in magnetic structural/depth model.

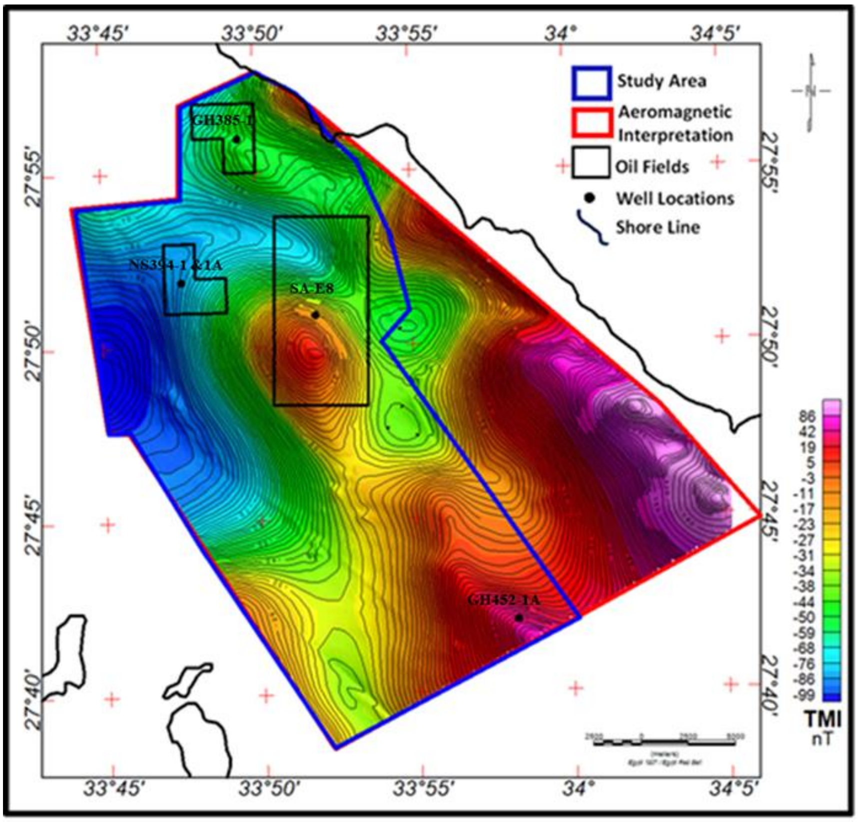

Fig. 5. Total Magnetic Field Intensity (TMI) map of South East Ghara, South Gulf of Suez, Egypt. The area of interest is shown within blue boundary (after CGG Company, 1997).

5. Results and discussions

5.1. Aeromagnetic data interpretation

5.1.1. Extracting signals of shallow and deep magnetic sources

The reduction to the magnetic pole (RTP) map (Fig. 6) is calculated from total magnetic field intensity (TMI) map (Fig. 5). RTP data is subjected to Gaussian filtering for depth slices to isolate and enhance the anomaly wavelengths associated with shallow (or deep) sources. Short-wavelength anomalies are produced by cultural sources and shallow geologic units, and longer-wavelength anomalies are produced by deeper geological units. This is done through applying power spectrum technique (Spector & Grant, 1970). The analysis of the produced power spectrum curve (Fig. 7) shows that, the deep-seated magnetic component frequencies vary from 0 to 0.07 cycles/grid unit, while the shallow magnetic component ranges from 0.07 to 0.7 cycles/grid. The deeper sources have an estimated average depth of 4.3 km, whereas the shallow sources have an average depth of 2.35 km as recorded in Table (1).

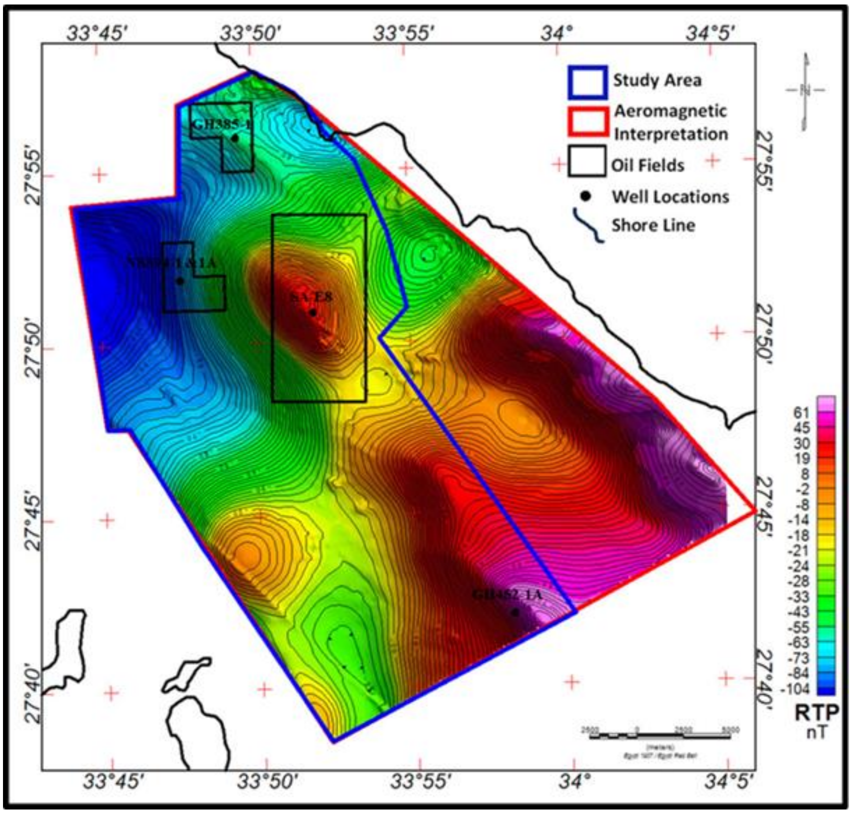

Fig. 6. Reduced to the North Magnetic Pole (RTP) of TMI, South East Ghara area, South Gulf of Suez, Egypt.

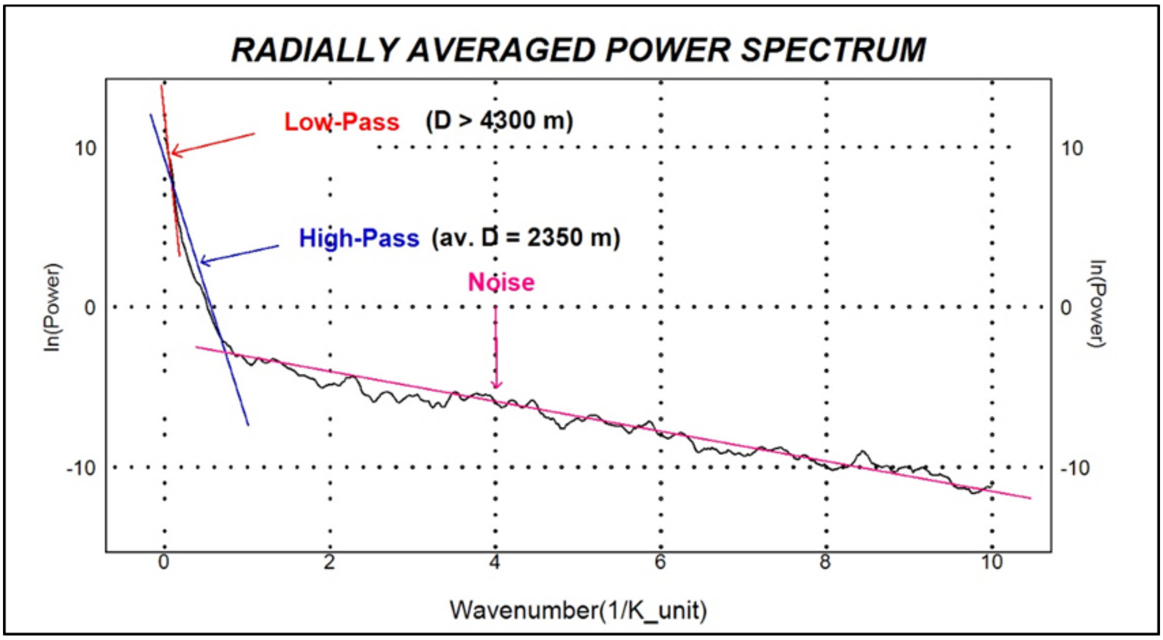

Fig. 7. Power spectrum of aeromagnetic data showing the corresponding averaging depths of South East Ghara area, South Gulf of Suez, Egypt.

Table 1. The level band components of aeromagnetic data of South East Ghara Area, South Gulf of Suez, Egypt.

Depth range	Depth slice (m)	Frequency band (Hz)	Wavelength range (km)
Deep	> 4300	< 0.0721	> 13.87
Shallow	(400 – 4300) Av. 2350	0.0721 – 0.711	1.4 – 13.87
Noise	< 400	> 0.7110	< 1.4

The cut-off wavenumber obtained from the intersection of the two lines is 0.072k (13.87). The low pass filtered aeromagnetic anomalies are shown in Figure 8. The low pass filtering was necessary to remove near surface effects. It can be concluded that low pass filtered aeromagnetic anomalies originate from a deep source that is larger than the surface outcrops. The residual aeromagnetic anomalies were high-pass filtered by using such cut-off wavenumber. The high-pass filtered aeromagnetic map shows concentric circular shaped anomalies are shown in Figure 9.

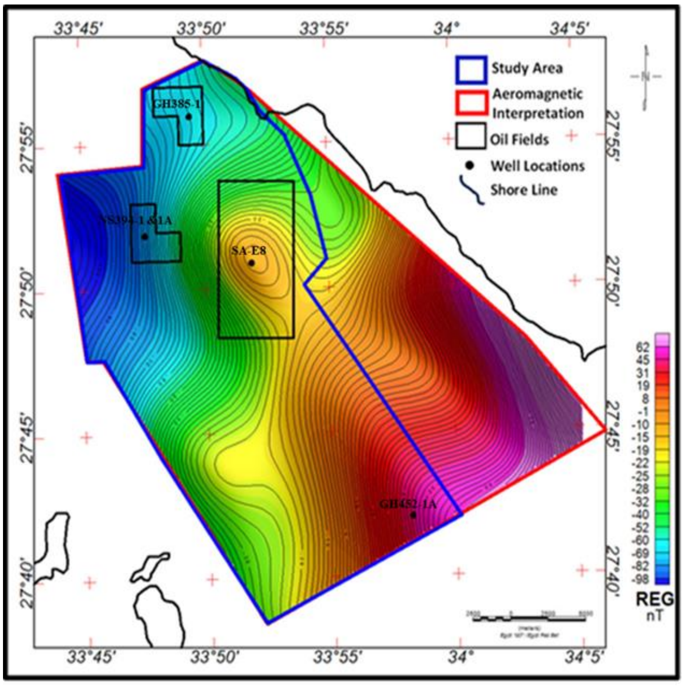

Fig. 8. Regional (Low-Pass, LP) aeromagnetic component at the deepest magnetic depth slice (4300 m) of South East Ghara area, South Gulf of Suez, Egypt.

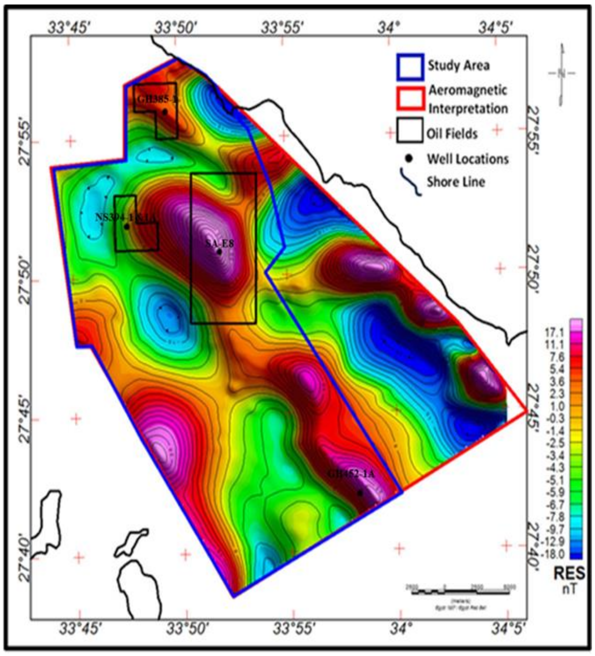

Fig. 9. Residual (High-Pass, HP) aeromagnetic component at shallower magnetic depth slice (av. 2320 m) of South East Ghara area, South Gulf of Suez, Egypt.

5.1.2. Basement structural and lineaments analysis

The first vertical and the tilt derivatives techniques are applied to RTP and its magnetic components data of the study area to amplify short-wavelength information and to emphasize edges of potential field sources. Figures (10 &11) show the vertical and the tilt derivatives maps of the residual component of RTP map. An integrated qualitative interpretation of the filtered magnetic components is used to construct the basement tectonics map (Fig. 12). These maps collectively indicated that the study area is dominated by NNW to NW oriented high basement structures (tilted-fault blocks) extending along the whole length of the area. These are alternating with parallel series of down-faulted basement block (fault-controlled basins). Both of high and low basement structures intensively dissected along their extensions by ENE-WSW oblique dip-slip and oblique-slip faults of different magnitudes of displacements.

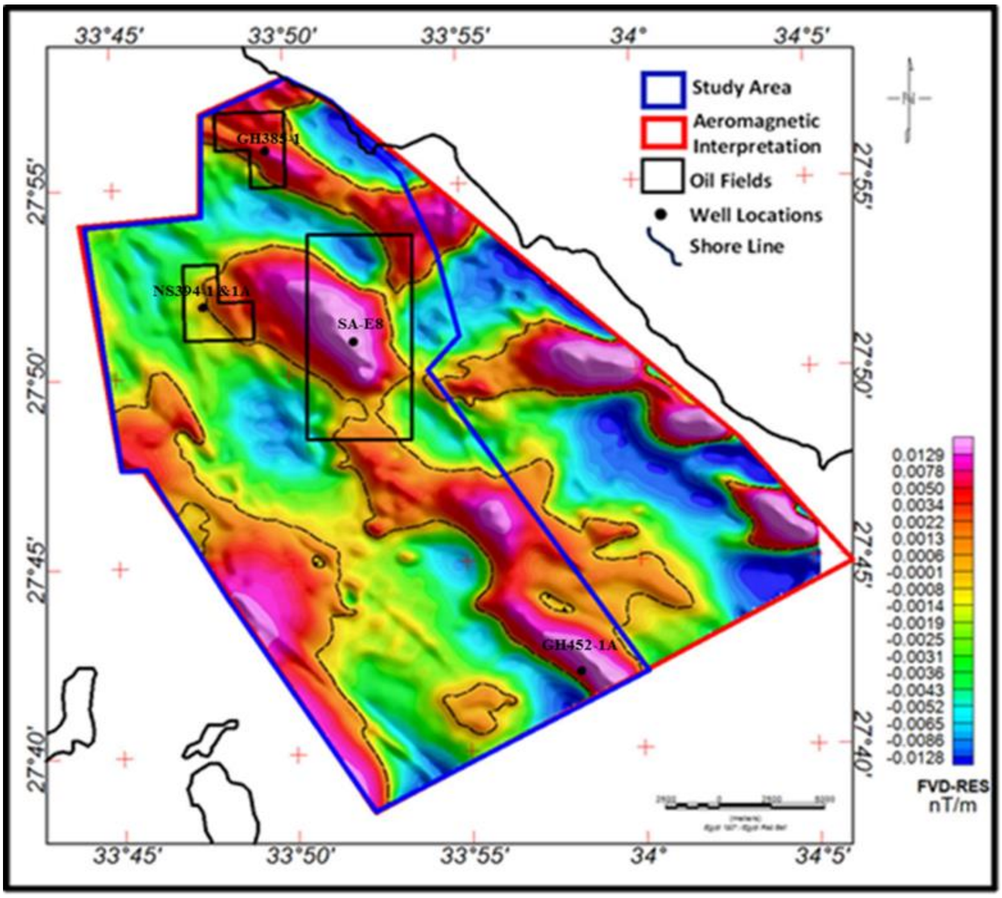

Fig. 10. First vertical derivative (FVD) of HP (Residual) RTP component of South East Ghara area, South Gulf of Suez, Egypt.

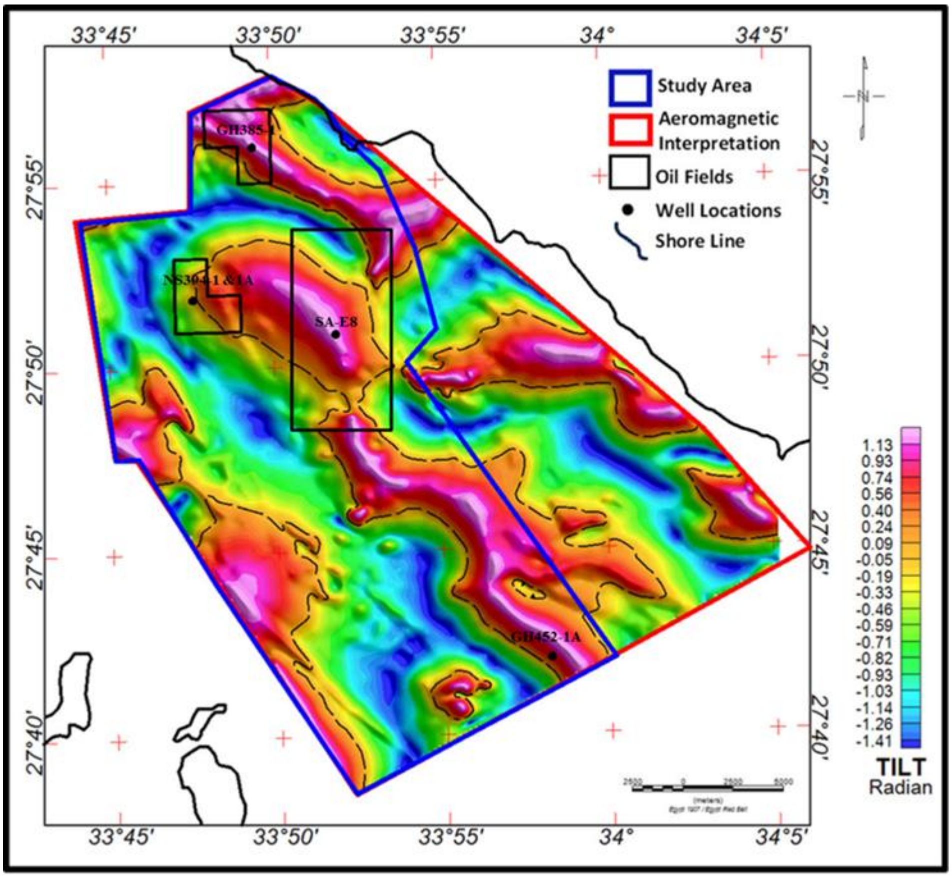

Fig. 11. Tilt derivative of HP (Residual) RTP component of South East Ghara area, South Gulf of Suez, Egypt.

A thorough analysis of magnetic anomaly bands on a basement level reveals numerous faults, horsts, and grabens (Fig. 12). The horst and graben structures have a general NNW-SSE structural trend. Structural elements detected from the combined RTP, high-pass and low-pass components (shallow and deep depth-slices), follow magnetic inflexion and are of dip-slip nature and others that follow lines of discontinuity, are of probable strike-slip nature. The trends of predominant faults across the study area are NNW-SSE to NW-SE and ENE-WSW to NE-SW. Figure (12) shows that the strike-slip faults have ENE-WSW to NE-SW trends, and represent younger faults, and the dip-slip faults are the main cause of the formation of the tilted faulted blocks have NNW-SSE to NW-SE directions. One of these tilted faulted block (which is affected significantly by the ENE-WSW strike-slip faults) forms the horst structure trend which separates between the Ghara basin and Eastern basin.

Two major sedimentary basins (grabens) were recognized and interpreted from magnetic data involves Ghara and Eastern basins (Fig. 12). These two basins have a general NNW-SSE trend. The ENE-WSW trending faults represented in the study area as crosscutting faults. These faults are interpreted as probable strike-slip faults; and extended across the area, and appear to mediate shallow saddle regions that separate narrower sub-basins in the central, from broader sub-basin developed in the study area (Fig. 12). This feature may be of comparable regional significance, especially as evidenced from its presence in the magnetic data.

Locally, based on the integrated qualitative interpretation of the filtered magnetic components, the estimated basement lithological units could be classified according to their average magnetic susceptibilities as following:

a. Non-magnetic lithology eg: Granitized terrain, carbonate meta-sediments; and/or down-faulted blocks.

b. Weakly magnetized lithology eg: Felsic intrusive or meta-intrusive, low-grade metasediment.

c. Moderately magnetic lithology eg: Intermediate intrusive or meta-intrusive, high grade metasediment.

d. Highly magnetized lithology eg: Mafic intrusive or meta-intrusive, sedimentary iron formation.

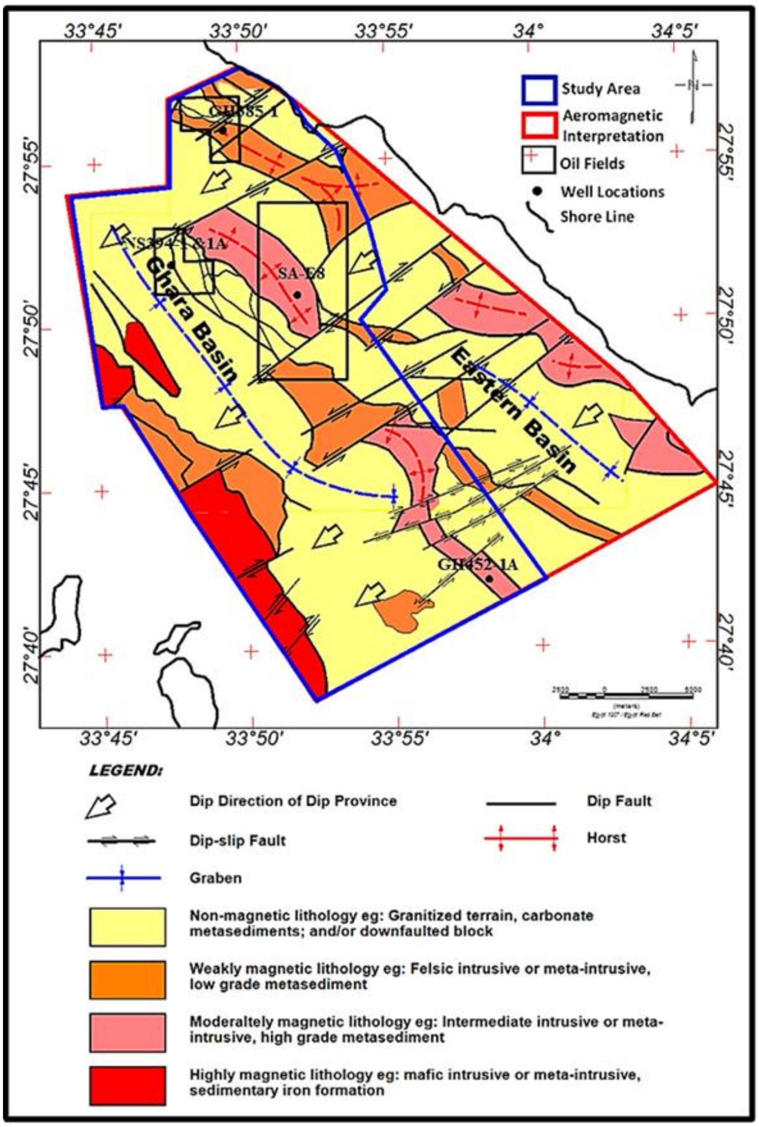

Fig. 12. Interpreted basement faults network as deduced from aeromagnetic data of South East Ghara area, South Gulf of Suez, Egypt.

5.2. 2D Seismic data interpretation

The study area shows a subsurface stratigraphic section includes the formations recognized of South East Ghara area. Some of these formations are picked, mapped and interpreted. This is performed by extract an arbitrary 2D-seismic line-oriented E-W and cross SA-E8 Well (Shoab Ali Oil Field) and NS394-1A (North Shedwan-3 Oil Field) (Fig. 13). Nine seismic reflectors are picked along this seismic line which are (basement, Nubia, Matulla, Nukhul, Rudeis, Kareem, Belayim, South Gharib and Zeit) as shown in Figure (13). The interpreted section reflects the presence of nine main clysmic normal faults (Cly. F1, Cly. F2, Cly. F3, Cly. F4, Cly. F5, Cly. F6, Cly. F7, Cly. F8 and Cly. F9), and two synthetic minor faults (Min. F1 and Min. F2). The nine faults have downthrow towards the SE direction and the synthetic faults have downthrow towards the same direction and form tilted fault blocks. Most of these faults dissect the Basement, Nubia, Matulla, Nukhul, Rudeis, Kareem and Belayim reflectors except Cly. F5, Cly. F6 do not dissect Kareem and Belayim, also Cly. F5 does not dissect Rudeis. Cly. F3 only dissects South Gharib reflector.

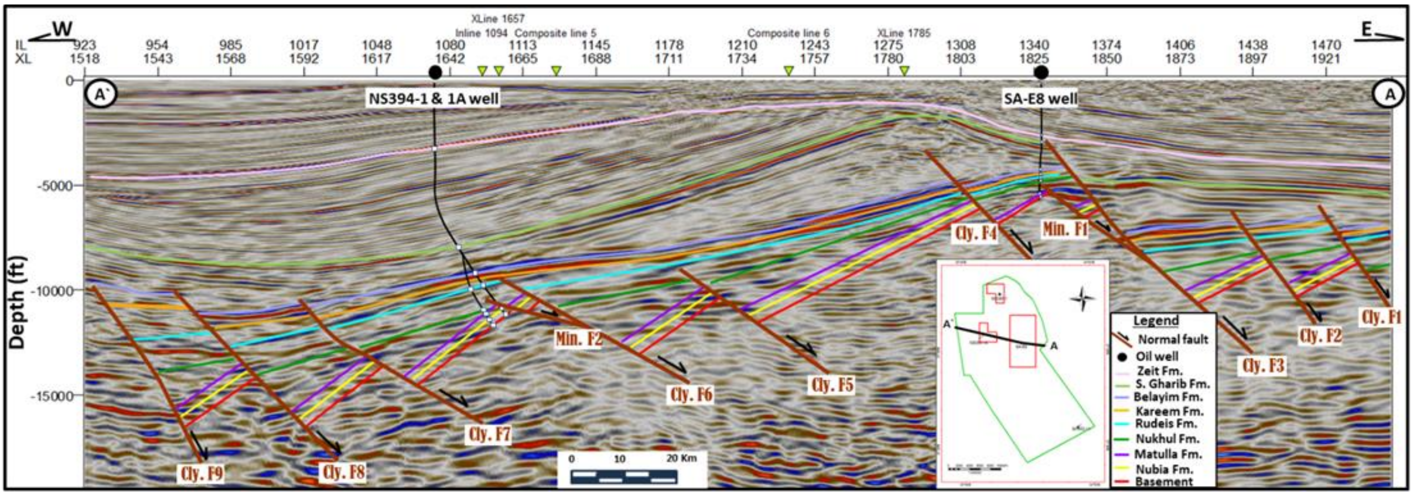

Fig. 13. Interpreted arbitrary 2D seismic line passing through SA-E8 Well (Shoab Ali Oil Field) and NS394-1 & 1A (North Shedwan-3 Oil Field) shows nine picked horizons and interpreted normal fault structure of South East Ghara area, South Gulf of Suez, Egypt.

Geo-seismic cross section of arbitrary line in the strike direction (NW-SE), passing through GH385-1 (North Shedwan-2 oil field), SA-E8 (Shoab Ali oil Field) and GH452-1A (Fig. 14) shows several interpreted horizons involve basement complex as well as Nubia, Matulla, Nukhul, Rudeis, Kareem, Belayim, South Gharib and Zeit formations in addition to post-Zeit sediments. It is characterized by the presence of one clysmic normal fault which is Cly. F3, and several of cross faults which are Cr. F1, Cr. F2, Cr. F3, Cr. F4, Cr. F5 and Cr. F6. These faults impacted the sequence resulted in the construction of the horst, graben structures and tilted fault blocks.

All these faults dissected the basement complex as well as Nubia, Matulla, Nukhul, Rudeis, Kareem, Belayim formations, where Cr. F2 dissected only the base of Belayim formation. South Gharib formation is dissected only by Cr. F6, while it is base dissected by all the faults except Cr. F2. The base of Zeit formation is dissected only by Cr. F6, while Post Zeit is not influenced by any Faults.

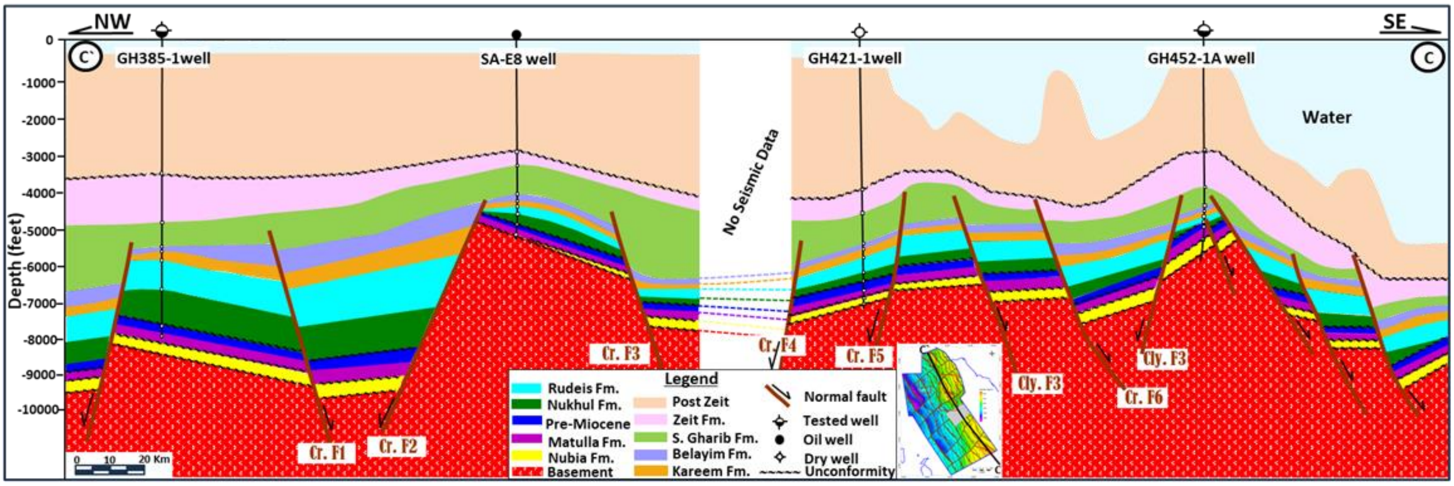

Fig. 14. Geo-Seismic Cross Section for Arbitrary line passing through GH385-1 (North Shedwan-2 oil field), SA-E8 (Shoab Ali oil Field) and GH452-1A, Based on 2D-Seismic Data of South East Ghara Area, South Gulf of Suez, Egypt.

The geo- seismic cross section is passing by four highs which are North Shedwan-2 oil field, Shoab Ali oil field, horst between SA-E8 & GH452-1A, and GH452-1A horst. Shoab Ali oil field and GH452-1A horst are almost leveled. The structure of area closed to the dry well (GH421-1) is separated by a structure saddle from Shoab Ali oil field. This structure is truncated to the south-east by northeasterly trending, down to the south young faults related to the post Miocene Red Sea pull apart.

5.3. Depth structural mapping

5.3.2. Depth structural mapping based on seismic data interpretation

The time maps of three key horizons (basement, Nubia and Matulla) are converted into depth maps using the average velocities. The depth structural contour maps of the three tops horizons (Figs. 15, 16 & 17) show two main fault trends, directed towards the NW-SE and NE-SW directions. There are observed that the basins mainly located in the western part of the study area. The trend of formations are mainly in NW-SE direction that are the result of Clysmic system. Noteworthy, Nubia and Matulla formations represent the source and reservoir rocks, while basement reservoir in the study area is represented only in Shoab Ali field.

The basement complex, Nubia, and Matulla formations are structurally controlled and get deeper in the northwest of the study area (North Shedwan-3) and shallower in the South East of the area, with interpreted depth values ranged from 16500, 16400, 14400 ft subsea in its deepest point and 4700, 4600, 4500 ft subsea in its shallowest point, respectively. The thickness of Nubia formation ranged from around 55-350 ft at the central part and the northwest of the study area, respectively, while the average thickness of Matulla formation is around 300 ft. Encountered thin Nubia formation below Matulla formation indicating that there is depositional variation (basement topography) and/or Pre-Miocene unconformity affecting Nubia sand thickness. Significant reduction in potential resource within the field due to footwall erosion. The sub-basins located in the western part is about 12.5 km wide and 60 km long, and bounded by the salt ridge in the southeast, and the uplifted offshore basement in the northwest.

Drilled wells data in South East Ghara show that the Nubia formation is a good reservoir with 36º API and average porosity 16% with Oil Water Contact (OWC) (- 10955 ft) at the northwest of the study area (North Shedwan-3). Also, Nubia formation produces with 36º API, porosity 19 % and OWC (-5450 ft) at Shoab Ali field. The Matulla formation is a good reservoir with 34º API and average porosity 19% with OWC (-5450 ft) at Shoab Ali field. Whereas fractured basement complex represents reservoir rocks with 31ºAPI and average porosity 15% in north shoab Ali field (E.G.P.C., (1996). Based on the well data and the structure analysis, there are observed that Nubia and Matulla formations involve 2 leads, (L1) (Figs. 16 & 17), with one prospect (P1) in Nubia formation and two prospects (P1 and P2) in Matulla formation as shown in Figures (16 & 17).

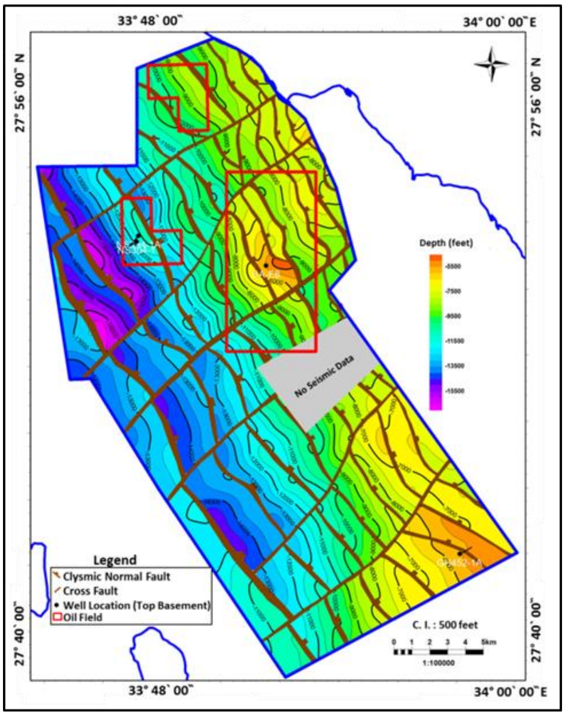

Fig. 15. Depth Structural contour map on the top of basement complex, based on 2D-seismic data of South East Ghara area, South Gulf of Suez, Egypt.

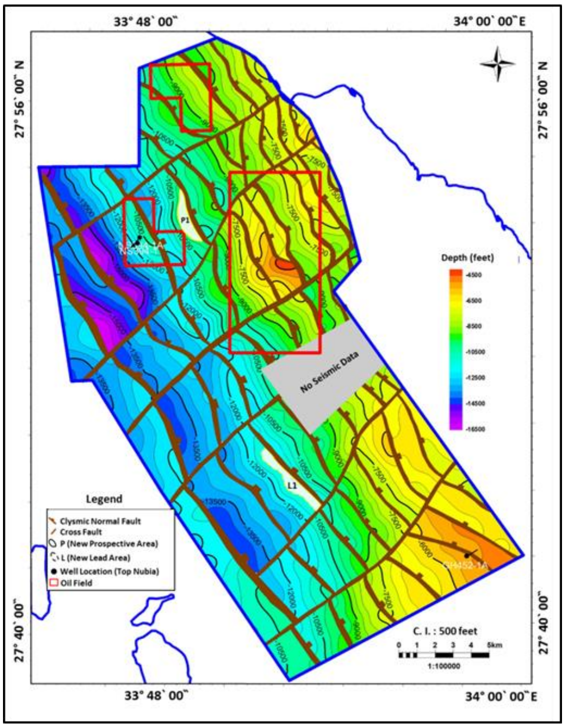

Fig. 16. Depth Structural Contour Map on the Top of Nubia Formation Based on 2D-Seismic Data of South East Ghara Area, South Gulf of Suez, Egypt.

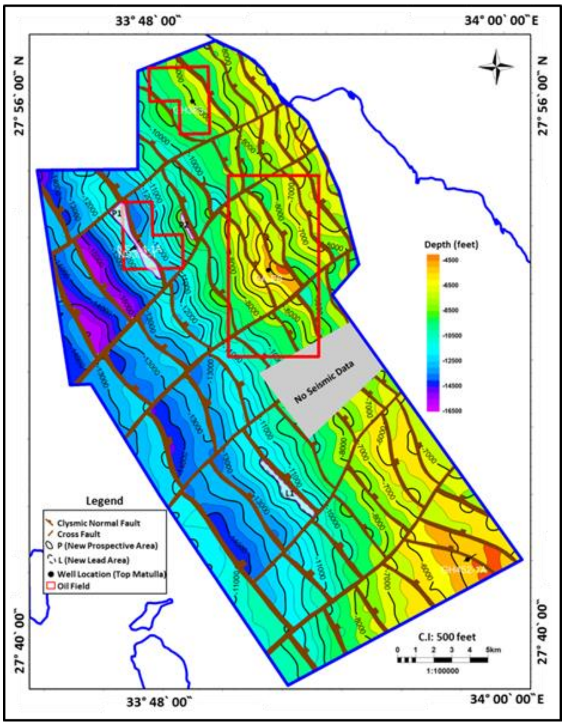

Fig. 17. Depth structural contour map of top of Matulla Formation based on 2D seismic data of South East Ghara area, South Gulf of Suez, Egypt.

Conclusion

The integrated aeromagnetic and seismic analysis show pre-rift and syn-rift sedimentary sections in the South East Ghara are structurally deformed with two main fault trends, directed towards the NW-SE and NE-SW directions with major trend NW-SE as a result of Clysmic system. This led to probable distribution patterns of hydrocarbon accumulations in the sedimentary basins. The basement complex is affected mainly by the intra-rifting major faults and the up-thrown side of these faults shows promising locations for hydrocarbon accumulations. Miocene evaporates may have served as a good seal for the stored hydrocarbon, giving it a good chance of accumulation. Based on the wells and structure analysis, the result suggest that Nubia and Matulla formations are a good reservoir involve promising localities represented in two leads, and three prospects, extended and distributed in the central and northwest of the study area.

Recommendation:

1. Drilling of an exploratory well in the new recommended prospect and lead areas, may throw more light on the lithological and structural setting of the area under consideration.
2. More studies on Matulla Formation at N. Shedwan-3 oil Field and following up its extension are needed.

References

Abd El-Naby, A., Abd El-Aal, M., Kuss, J., Bokhary, M. and Lashin, A., (2009) Structural and basin evolution in Miocene time, southwestern Gulf of Suez, Egypt. – N. Jb. Geol. Paläont. Abh., **251**, 331– 353; Stuttgart.

Abd-Allah, A. M., Aal, M. H. A., El-Said, M. M. and Abd El-Naby, A., (2014) Structural evolution of the southern transfer zone of the Gulf of Suez rift, Egypt. Journal of African Earth Sciences, **96**, 21-38.

Alsharhan, A. S., (2003) Petroleum geology and potential hydrocarbon plays in the Gulf of Suez rift basin, Egypt. AAPG bulletin, **87**(1), 143-180.

Barakat, M. G., (1982) General review of the petroliferous provinces of Egypt with special emphasis on their geological setting and oil potentialities. – **87** pp.; unpubl. rep.; Geology Department,

Bosworth, W. and Durocher, S., (2017) Present-day stress fields of the Gulf of Suez (Egypt) based on exploratory well data: non-uniform regional extension and its relation to inherited structures and local plate motion. Journal of African Earth Sciences, **136**, 136-147.

Bosworth, W. and McClay, K. R., (2001) Structural and stratigraphic evolution of the Gulf of Suez Rift, Egypt: a synthesis: In: Zeigler, P. A., Cavazza, W., Robertson, A. H. F., Crasquin-Soleau, S. (Eds.), Peri-

Tethyan Rift-Wrench Basins and Passive Margins. Musee Nationale Hist. Nat., 567 - 606.

BP/GUPCO, (2013) Pre-Stack Time Migration Report for Hilal North Shedwan PSTM, By Western Geco.

CGG., (1997) High-resolution aeromagnetic.

E.G.P.C., (1996) "Gulf of Suez Oil Field" A Comprehensive Overview, Cairo, Egypt. **736** p.

E.G.P.C., (2023) Egypt oil and gas concession map, February, 2023.

El Diasty, W. S., El Beialy, S. Y., Mostafa, A. R., Abo Ghonaim, A. A. and Peters, K. E., (2020) Chemometric differentiation of oil families and their potential source rocks in the Gulf of Suez. Natural Resources Research, **29**, 2063 - 2102.

Gawthorpe, R. L., Hurst, J. M. and Sladen, C. P., (1990) Evolution of Miocene footwall-derived coarse-grained deltas, Gulf of Suez, Egypt: implications for exploration: AAPG Bulletin, v. **74**, 1077 - 1086.

Geosoft Inc., (2008): Magmap, 2-D frequency domain processing. Geosoft Inc., Toronto, Canada, 34.

GUPCO, (1982) Internal report of post appraisal of GH385-1 well, Cairo, Egypt.

GUPCO, (1984): Internal report of post appraisal report of GH452-1A well, Cairo, Egypt.

GUPCO, (2007) Internal report of post appraisal of NS394-1A well, Cairo, Egypt.

GUPCO, (2013) Internal report of final well report of NS394-4 well, Cairo, Egypt.

Harper, M. L., (1966) Block faulting and sedimentation in the Gulf of Suez. – Unpublished internal company report, **36** p.

Meshref, W. M., Refai, E. and Abd El Baki, S., (1976) Structural interpretation of the Gulf of Suez and its oil potentialities. - unpublished report; EGPC, 5th Exploration Seminar, Cairo.

Patton, T. L., Moustafa, A. R., Nelson, R. A. and Abdine, A. S., (1994) Tectonic evolution and structural setting of the Gulf of Suez rift, Egypt: In Interior Rift basins, S.M. Landon (Editor), AAPG Memoir, no. **59**, 9 - 55.

Radwan, A. E. and Sen, S., (2021) Characterization of in-situ stresses and its implications for production and reservoir stability in the depleted El Morgan hydrocarbon field, Gulf of Suez Rift Basin, Egypt. Journal of Structural Geology, **148**, p.104355.

Radwan, A. E., (2018) New petrophysical approach and study of the pore pressure and formation damage in Badri, Morgan and Sidki fields, Gulf of Suez Region Egypt: PhD Thesis (2018). https:// doi.org/10.13140/RG.2.2.26651.82727.

Radwan, A. E., Kassem, A. A. and Kassem, A., (2020) Radwany Formation: A new formation name for the Early-Middle Eocene carbonate sediments of the offshore October oil field, Gulf of Suez: Contribution to the Eocene sediments in Egypt. Marine and Petroleum Geology, **116**, p.104304.

Radwan, A. E., Rohais, S. and Chiarella, D., (2021) Combined stratigraphic structural play characterization in hydrocarbon exploration: a case study of Middle Miocene sandstones, Gulf of Suez basin. Egypt. J. Asian Earth Sci. (2021). https://doi.org/10.1016/j.jse aes.2021.104686.

Rohais, S., Barrois, A., Colletta, B. and Moretti, I., (2016) Pre-salt to salt stratigraphic architecture in a rift basin: insights from a basin-scale study of the Gulf of Suez (Egypt). Arabian Journal of Geosciences, **9**, 1 - 24.

Said, R., (1962) The Geology of Egypt. El Sevier publishing, Amsterdam - New York, 407 - 411.

Schlumberger, (1984) Well Evaluation Conference, Egypt Schlumberger Ltd., 18 - 26.

Schlumberger, (2017) Petrel Software for Seismic interpretation.

Segev, A., Avni, Y., Shahar, J. and Wald, R., (2017) Late Oligocene and Miocene different seaways to the Red Sea–Gulf of Suez rift and the Gulf of Aqaba–Dead Sea basins. Earth-science reviews, **171**, 196 - 219.

Sharp, I. R., Gawthorpe, R. L., Armstrong, B. and Undrhill, J. R., (2000b) Propagation history and passive rotation of mesoscale normal faults: REFERENCE 230 implications for syn-rift stratigraphic development: Basin Research, **12**, 285 - 306.

Sharp, I. R., Gawthorpe, R. L., Undrhill, J. R. and Gupta, S., 2000a. Fault-propagation folding in extensional settings: Examples of structural style and syn-rift sedimentary response from the Suez Rift, Sinai, Egypt: Geological Society of America Bulletin, **112**, 1877 - 1899.

Spector, A., and Grant, F. S., (1970) Statistical models for interpreting aeromagnetic data. Geophysics, V. **35**, 293 – 302.

Temraz, M. and Dypvik, H., (2018) The lower Miocene Nukhul Formation (Gulf of Suez, Egypt): microfacies and reservoir characteristics. Journal of Petroleum Exploration and Production Technology, **8**, 85 - 98.

Tromp, S. W., (1950) The age and origin of the Red Sea Graben. Geological Magazine, **87**, 385 - 392.